

Dilatation part of the phonon-electron interaction and phonon conductivity of lightly doped silicon and germanium

M. K. Roy* and K. C. Sood

Department of Physics, Banaras Hindu University, Varanasi 221 005, India

(Received 14 July 1992)

The nonspherical nature of the donor wave function is taken into account for the derivation of electron-phonon rates in Li-O-doped Si. It is also found that the nonzero dilatational part of the anisotropic (longitudinal) phonon-electron scattering cross section is capable of explaining the thermal conductivity beyond its maximum, both for Si and Ge doped with shallow donors.

I. INTRODUCTION

Recently we have developed a theory¹ for the use of anisotropic form factor in the phonon-electron relaxation rate, τ_{e-ph}^{-1} , in semiconductors with shallow donors and showed that it can improve the theoretical explanation of the low-temperature phonon-transport data² in some cases, e.g., As-doped Ge. This improvement was a consequence of the increase in the cutoff frequency for τ_{e-ph}^{-1} . The theory revealed that the contribution due to the dilatation part of the deformation potential matrix to τ_{e-ph}^{-1} is not zero. Calculations for its explicit effect on phonon conductivity, however, were not performed. There was still some overestimation in the phonon conductivity results beyond $T=6$ K and various possibilities, which could be responsible for this, were discussed qualitatively.

In an attempt to explore the cause for this discrepancy, we first extend our theory to higher temperatures and almost unexpectedly achieve a satisfactory explanation of phonon transport in As-doped Ge from $T=30$ to 100 K. In order to observe the effect of anisotropy elsewhere, we have picked up the case of the Li-O donor in Si for which the chemical shift $4\Delta=7.7$ meV, corresponding to the resonance frequency $\omega_r=1.17 \times 10^{13}$ Hz. This value is higher than the cutoff frequency ($\approx 3.67 \times 10^{12}$ Hz) defined by $qa^*=1$ in the isotropic model; a^* , equal to 17.16 Å in Si with shallow donors, is the effective Bohr radius. Anisotropy of the form factor, as mentioned earlier, increases the cutoff frequency and so our theory might show some effects in this case also. Even though the anisotropy of the donor wave function in this case is not as large as in the case of n -type Ge; still, due to the nonavailability of experimental data of κ for a system with larger anisotropy, we are left with no other choice. In Sec. II, we derive the expressions for τ_{e-ph}^{-1} for n -type Si. In Sec. III, the theory is applied to Li-O-doped Si as well as As-doped Ge and the results are discussed with an emphasis towards the role of E_d on phonon conductivity at higher temperatures. Possible reasons for the remaining discrepancy around the conductivity peak have also been pointed out.

II. THEORY

Phonon-electron relaxation rates: All expressions of τ_{e-ph}^{-1} for As-doped Ge can be found in Ref. 1 and there-

fore only the case of Li-O donors in Si will be presented here. Li-O donors in Si³, as any other group-V donors, have T_d site symmetry. The sixfold donor ground state, due to valley-orbit interaction, split up into $1s(A_1)$ singlet and $1s(E+T_2)$ fivefold degenerate states. The corresponding wave function is written as⁴

$$\Psi_s(\mathbf{r}) = \sum_{j=1}^6 \alpha_s^j F^j(\mathbf{r}) \Phi^j(\mathbf{r}). \tag{1}$$

The values of α_s^j and the hydrogenlike envelope function $F^j(\mathbf{r})$ can be found in Ref. 4. $\Phi^j(\mathbf{r})$ is the Bloch function in the j th minimum of the conduction band. According to Cheung and Barrie,⁵ the electron-phonon matrix element is found to be

$$\Omega_{mn}^{q\lambda} = i \left[\frac{\hbar q}{2\rho V v_\lambda} \right]^{1/2} \sum_{j=1}^6 \theta_{1s,1s}^j(\mathbf{q}) A_{mn}^j(\mathbf{q}, \lambda), \tag{2}$$

where

$$A_{mn}^j(\mathbf{q}, \lambda) = \alpha_m^j \alpha_n^j \{ E_d \delta_{\lambda,1} + E_u e_\lambda(\mathbf{q}) (\hat{\mathbf{k}}^{(j)} \hat{\mathbf{k}}^{(j)}) e_1(\mathbf{q}) \}$$

and

$$\theta_{1s,1s}^j(\mathbf{q}) = \left[1 + \left[\frac{qa}{2} \right]^2 - (a^2 - b^2) \frac{q^2}{4} \cos^2 \theta_j \right]^{-2}.$$

Here all terms have the same meaning as Ref. 1. $\theta_{1s,1s}^j(q)$ is the anisotropic form factor. The values of the dyad $(\hat{\mathbf{k}}^{(j)} \hat{\mathbf{k}}^{(j)})$ for different j in Si are given in Table I. The values of a and b can be calculated by the method given in Ref. 6. Also some relations between the deformation

TABLE I. Values of $\hat{\mathbf{k}}^{(j)} \hat{\mathbf{k}}^{(j)}$ for different j in silicon.

$(\hat{\mathbf{k}}^{(1)} \hat{\mathbf{k}}^{(1)}) = (\hat{\mathbf{k}}^{(2)} \hat{\mathbf{k}}^{(2)}) =$	$\begin{bmatrix} 1 & 0 & 0 \\ 0 & 0 & 0 \\ 0 & 0 & 0 \end{bmatrix}$
$(\hat{\mathbf{k}}^{(3)} \hat{\mathbf{k}}^{(3)}) = (\hat{\mathbf{k}}^{(4)} \hat{\mathbf{k}}^{(4)}) =$	$\begin{bmatrix} 0 & 0 & 0 \\ 0 & 1 & 0 \\ 0 & 0 & 0 \end{bmatrix}$
$(\hat{\mathbf{k}}^{(5)} \hat{\mathbf{k}}^{(5)}) = (\hat{\mathbf{k}}^{(6)} \hat{\mathbf{k}}^{(6)}) =$	$\begin{bmatrix} 0 & 0 & 0 \\ 0 & 0 & 0 \\ 0 & 0 & 1 \end{bmatrix}$

potential matrices $A_{mn}^j(\mathbf{q}, \lambda)$, which would be useful for the calculations of τ_{e-ph}^{-1} , have been derived to be as follows:

$$\begin{aligned}
A_{11}^j(\mathbf{q}, \lambda) &= A_{00}^j(\mathbf{q}, \lambda) - \frac{1}{\sqrt{2}} A_{01}^j(\mathbf{q}, \lambda), \\
A_{22}^j(\mathbf{q}, \lambda) + A_{00}^j(\mathbf{q}, \lambda) &+ \frac{1}{\sqrt{2}} A_{01}^j(\mathbf{q}, \lambda), \\
A_{33}^j(\mathbf{q}, \lambda) &= A_{00}^j(\mathbf{q}, \lambda) + \frac{1}{\sqrt{2}} A_{01}^j(\mathbf{q}, \lambda) - \sqrt{3/2} A_{02}^j(\mathbf{q}, \lambda), \\
A_{44}^j(\mathbf{q}, \lambda) &= A_{00}^j(\mathbf{q}, \lambda) + \frac{1}{\sqrt{2}} A_{01}^j(\mathbf{q}, \lambda) + \sqrt{3/2} A_{02}^j(\mathbf{q}, \lambda), \\
A_{55}^j(\mathbf{q}, \lambda) &= A_{00}^j(\mathbf{q}, \lambda) - \sqrt{2} A_{01}^j(\mathbf{q}, \lambda), \\
A_{12}^j(\mathbf{q}, \lambda) &= \frac{1}{\sqrt{2}} A_{02}^j(\mathbf{q}, \lambda), \quad A_{13}^j(\mathbf{q}, \lambda) = \frac{1}{\sqrt{2}} A_{03}^j(\mathbf{q}, \lambda) \\
A_{14}^j(\mathbf{q}, \lambda) &= \frac{1}{\sqrt{2}} A_{04}^j(\mathbf{q}, \lambda), \quad A_{15}^j(\mathbf{q}, \lambda) = -\sqrt{2} A_{05}^j(\mathbf{q}, \lambda) \\
A_{23}^j(\mathbf{q}, \lambda) &= -\sqrt{3/2} A_{03}^j(\mathbf{q}, \lambda), \\
A_{24}^j(\mathbf{q}, \lambda) &= \sqrt{3/2} A_{04}^j(\mathbf{q}, \lambda),
\end{aligned} \tag{3}$$

$$A_{25}^j(\mathbf{q}, \lambda) = 0,$$

$$A_{34}^j(\mathbf{q}, \lambda) = 0,$$

$$A_{35}^j(\mathbf{q}, \lambda) = 0,$$

$$A_{45}^j(\mathbf{q}, \lambda) = 0.$$

Adopting the same procedure as given in Refs. 1 and 7-9, we obtain the following expressions for the phonon-electron relaxation rates corresponding to various processes.

(i) Elastic scattering off the singlet $1s(A_1)$ state:

$$\begin{aligned}
\tau_{q\lambda}^{-1}(\text{el}, 0) &= \frac{N_0 \omega_{q\lambda}^4}{4\pi\rho^2 v_\lambda^2} \\
&\times \sum_{\lambda'} \frac{1}{v_{\lambda'}^5} \frac{4(4\Delta)^2}{\{(\hbar\omega_{q\lambda})^2 - (4\Delta)^2\}^2 + 4\Gamma^2(4\Delta)^2} \\
&\times \sum_{m=1}^5 \langle (M_{0m}^{q'\lambda'})^2 \rangle \langle (M_{m0}^{q\lambda})^2 \rangle. \tag{4}
\end{aligned}$$

(ii) Elastic scattering off the $1s(E + T_2)$ state:

$$\begin{aligned}
\tau_{q\lambda}^{-1}(\text{el}, 5) &= \frac{N_1 \omega_{q\lambda}^4}{4\pi\rho^2 v_\lambda^2} \sum_{\lambda'} \frac{1}{v_{\lambda'}^5} \left[\frac{4(4\Delta)^2}{\{(\hbar\omega_{q\lambda})^2 - (4\Delta)^2\}^2 + 4\Gamma^2(4\Delta)^2} \sum_{m=1}^5 \langle (M_{0m}^{q'\lambda'})^2 \rangle \langle (M_{m0}^{q\lambda})^2 \rangle \right. \\
&\quad \left. + \frac{2(4\Delta)^2 \{(\hbar\omega_{q\lambda})^2 + (4\Delta)^2\}}{[\{(\hbar\omega_{q\lambda})^2 - (4\Delta)^2\}^2 + 4\Gamma^2(4\Delta)^2] (\hbar\omega_{q\lambda})^2} \sum_{n=1}^5 \langle (M_{0n}^{q'\lambda'})^2 \rangle \sum_{\substack{m=1 \\ m \neq n}}^5 \langle (M_{m0}^{q\lambda})^2 \rangle \right]. \tag{5}
\end{aligned}$$

(iii) Inelastic scattering from the $1s(E + T_2)$ states to the $1s(A_1)$ state:

$$\begin{aligned}
\tau_{q\lambda}^{-1}(\text{inel}) &= \frac{N_1 \omega_{q\lambda}}{4\pi\rho^2 v_\lambda^2} \sum_{\lambda'} \frac{(4\Delta/\hbar + \omega_{q\lambda})^3}{v_{\lambda'}^5} \left[\frac{1}{\hbar\omega_{q\lambda}} - \frac{1}{\hbar\omega_{q\lambda} + 4\Delta} \right]^2 \\
&\times \left[\frac{1}{2} \langle (M_{01}^{q'\lambda'})^2 \rangle \langle (M_{10}^{q\lambda})^2 \rangle + \frac{1}{2} \langle (M_{02}^{q'\lambda'})^2 \rangle \langle (M_{20}^{q\lambda})^2 \rangle + 2 \langle (M_{03}^{q'\lambda'})^2 \rangle \langle (M_{30}^{q\lambda})^2 \rangle \right. \\
&\quad + 2 \langle (M_{04}^{q'\lambda'})^2 \rangle \langle (M_{40}^{q\lambda})^2 \rangle + 2 \langle (M_{05}^{q'\lambda'})^2 \rangle \langle (M_{50}^{q\lambda})^2 \rangle \\
&\quad + \langle (M_{10}^{q\lambda})^2 \rangle \left\{ \frac{1}{2} \langle (M_{02}^{q'\lambda'})^2 \rangle + \frac{1}{2} \langle (M_{03}^{q'\lambda'})^2 \rangle + \frac{1}{2} \langle (M_{04}^{q'\lambda'})^2 \rangle + 2 \langle (M_{05}^{q'\lambda'})^2 \rangle \right\} \\
&\quad + \langle (M_{20}^{q\lambda})^2 \rangle \left\{ \frac{1}{2} \langle (M_{01}^{q'\lambda'})^2 \rangle + \frac{3}{2} \langle (M_{03}^{q'\lambda'})^2 \rangle + \frac{3}{2} \langle (M_{04}^{q'\lambda'})^2 \rangle \right\} \\
&\quad + \langle (M_{30}^{q\lambda})^2 \rangle \left\{ \frac{1}{2} \langle (M_{01}^{q'\lambda'})^2 \rangle + \frac{3}{2} \langle (M_{02}^{q'\lambda'})^2 \rangle \right\} \\
&\quad + \langle (M_{40}^{q\lambda})^2 \rangle \left\{ \frac{1}{2} \langle (M_{01}^{q'\lambda'})^2 \rangle + \frac{3}{2} \langle (M_{02}^{q'\lambda'})^2 \rangle \right\} + 2 \langle (M_{50}^{q\lambda})^2 \rangle \langle (M_{01}^{q'\lambda'})^2 \rangle \left. \right] \\
&\times \left[1 - \exp \left[-\frac{\hbar\omega_{q\lambda}}{k_B T} \right] \right] \left[1 - \exp \left[\frac{-4\Delta - \hbar\omega_{q\lambda}}{k_B T} \right] \right]^{-1}. \tag{6}
\end{aligned}$$

(iv) Thermally assisted phonon absorption from the $1s(A_1)$ to $1s(E + T_2)$ states:

$$\begin{aligned}
\tau_{q\lambda}^{-1}(\text{ab}) &= \frac{N_0 \omega_{q\lambda}}{4\pi\rho^2 v_\lambda^2} \sum_{\lambda'} \frac{|4\Delta/\hbar - \omega_{q\lambda}|^3}{v_{\lambda'}^5} \left[\frac{1}{\hbar\omega_{q\lambda}} + \frac{1}{4\Delta - \hbar\omega_{q\lambda}} \right]^2 \\
&\times \left[\frac{1}{2} \langle (M_{10}^{q\lambda})^2 \rangle \langle (M_{01}^{q'\lambda'})^2 \rangle + \frac{1}{2} \langle (M_{02}^{q'\lambda'})^2 \rangle \langle (M_{20}^{q\lambda})^2 \rangle + 2 \langle (M_{03}^{q'\lambda'})^2 \rangle \langle (M_{30}^{q\lambda})^2 \rangle \right. \\
&\quad + 2 \langle (M_{04}^{q'\lambda'})^2 \rangle \langle (M_{40}^{q\lambda})^2 \rangle + 2 \langle (M_{05}^{q'\lambda'})^2 \rangle \langle (M_{50}^{q\lambda})^2 \rangle \\
&\quad + \langle (M_{10}^{q\lambda})^2 \rangle \left\{ \frac{1}{2} \langle (M_{02}^{q'\lambda'})^2 \rangle + \frac{1}{2} \langle (M_{03}^{q'\lambda'})^2 \rangle + \frac{1}{2} \langle (M_{04}^{q'\lambda'})^2 \rangle + 2 \langle (M_{05}^{q'\lambda'})^2 \rangle \right\} \\
&\quad + \langle (M_{20}^{q\lambda})^2 \rangle \left\{ \frac{1}{2} \langle (M_{01}^{q'\lambda'})^2 \rangle + \frac{3}{2} \langle (M_{03}^{q'\lambda'})^2 \rangle + \frac{3}{2} \langle (M_{04}^{q'\lambda'})^2 \rangle \right\} \left. \right]
\end{aligned}$$

$$\begin{aligned}
& + \langle (M_{30}^{q\lambda})^2 \rangle \left\{ \frac{1}{2} \langle (M_{01}^{q'\lambda'})^2 \rangle + \frac{3}{2} \langle (M_{02}^{q'\lambda'})^2 \rangle \right\} \\
& + \langle (M_{40}^{q\lambda})^2 \rangle \left\{ \frac{1}{2} \langle (M_{01}^{q'\lambda'})^2 \rangle + \frac{3}{2} \langle (M_{02}^{q'\lambda'})^2 \rangle \right\} + 2 \langle (M_{01}^{q'\lambda'})^2 \rangle \langle (M_{30}^{q\lambda})^2 \rangle \\
& \times \left[1 - \exp \left[-\frac{\hbar\omega_{q\lambda}}{k_B T} \right] \right] \left[\left[\exp \left[\frac{4\Delta - \hbar\omega_{q\lambda}}{k_B T} \right] - 1 \right] \right]^{-1}. \quad (7)
\end{aligned}$$

In all the above equations N_0 and N_1 are the density of electrons in the $1s(A_1)$ and $1s(E+T_2)$ states, respectively, where

$$N_0 = f_0(T)N_{ex}, \quad N_1 = f_0(T)\exp(-4\Delta/k_B T)N_{ex},$$

$$f_0(T) = [1 + 5 \exp(-4\Delta/k_B T)]^{-1}.$$

Combining Eqs. (4)–(7), we get

$$\tau_{e-ph}^{-1} = \tau_{q\lambda}^{-1}(el, 0) + \tau_{q\lambda}^{-1}(el, 5) + \tau_{q\lambda}^{-1}(inel) + \tau_{q\lambda}^{-1}(ab). \quad (8)$$

In expression (7), a singularity occurs at resonance, where $\hbar\omega_{q\lambda} = 4\Delta$. A level width could be added with $(\hbar\omega_{q\lambda} - 4\Delta)$ in the denominator to remove this singularity. Kowk⁸ has, however, used the more sophisticated Green's-function technique to provide the following expression of $\tau_{q\lambda}^{-1}(ab)$:

$$\begin{aligned}
\tau_{q\lambda}^{-1}(\text{resonance}) &= \frac{N_0 \omega_{q\lambda}}{\rho v_\lambda^2} \left[1 - \exp \left[-\frac{\hbar\omega_{q\lambda}}{k_B T} \right] \right] \\
&\times \sum_{m=1}^5 \langle (M_{0m}^{q\lambda})^2 \rangle \\
&\times \frac{\Gamma_0 + \Gamma_p}{(4\Delta + \hbar\omega_{q\lambda})^2 + (\Gamma_0 + \Gamma_p)^2}. \quad (9)
\end{aligned}$$

Therefore, to avoid singularity near resonance we should replace Eq. (7) by (9). In Eqs. (4), (5), and (9), Γ_0 and Γ_p are the level width of the $1s(A_1)$ and $1s(E+T_2)$ states, respectively. Following Kowk⁸ we can write (neglecting splitting of the fivefold degenerate state)

$$\begin{aligned}
\Gamma_0 &= \frac{1}{4\pi\rho} \left[\frac{4\Delta}{\hbar} \right]^3 \\
&\times \sum_{\lambda} \frac{1}{v_\lambda^5} \langle (M_{10}^{q\lambda})^2 \rangle \left[\exp \left[\frac{4\Delta}{k_B T} \right] - 1 \right]^{-1}, \quad (10a)
\end{aligned}$$

$$\begin{aligned}
\Gamma_p &= \frac{1}{4\pi\rho} \left[\frac{4\Delta}{\hbar} \right]^3 \\
&\times \sum_{\lambda} \frac{1}{v_\lambda^5} \langle (M_{10}^{q\lambda})^2 \rangle \left[1 - \exp \left[-\frac{4\Delta}{k_B T} \right] \right]^{-1}, \quad (10b)
\end{aligned}$$

and the total level width Γ is

$$\begin{aligned}
\Gamma &= \Gamma_0 + \Gamma_p = \frac{1}{4\pi\rho} \left[\frac{4\Delta}{\hbar} \right]^3 \left[1 + \frac{2}{\exp(4\Delta/k_B T) - 1} \right] \\
&\times \sum_{\lambda} \frac{\langle (M_{10}^{q\lambda})^2 \rangle}{v_\lambda^5}. \quad (10c)
\end{aligned}$$

III. RESULTS AND DISCUSSION

Table II provides all the parameters used for the calculations of phonon conductivity given by¹⁰

$$\kappa = \kappa_l(02) + \sum_{t=t_1 t_2} \{ \kappa_t(01) + \kappa_t(12) \}, \quad (11)$$

where

$$\begin{aligned}
\kappa_\lambda(nm) &= \frac{k_B}{6\pi^2 v_{g\lambda}(nm)} \left\{ \frac{k_B T}{\hbar} \right\}^3 \\
&\times \int_{\theta_n/T}^{\theta_m/T} \tau_c(\lambda, x) x^4 e^x (e^x - 1)^{-2} dx \quad (11a)
\end{aligned}$$

and

$$\begin{aligned}
\tau_c^{-1}(\lambda) &= \tau_B^{-1} + \tau_{pt}^{-1} + \tau_{e-ph}^{-1}(\lambda) \\
&+ \tau_N^{-1}(\lambda) + \tau_U^{-1}(\lambda). \quad (11b)
\end{aligned}$$

All expressions for various relaxation rates and their parameters, phonon velocities, limits of integrals, etc., can be found in Refs. 1 and 10. For Ge, $\tau_{e-ph}^{-1}(\lambda)$ are reported in Ref. 1 while for Si, they are given in the theory section of this paper. The values of a and b are calculated from Eq. (6) of Ref. 1 for which the required values of m_t , m_t , and the ionization energies are available in Refs. 1 and 11.

Figures 1 and 2 show the comparison between the best fit obtained from our theory with that of the isotropic model.^{7,11} In the case of As-doped Ge, the required values of $E_d = -4.0$ and -9.0 eV for the two samples are not far from the values reported earlier.^{13,14} During the calculations it was observed that the choice of E_d was very difficult and even a little experimental error in the

TABLE II. Values of the parameters used in the calculation of phonon conductivity.

Sample	N_{ex} in cm^{-3}	L_c in cm	4Δ in MeV	e_u in eV	E_d in eV
Ge-1	2.1×10^{16}	0.276	4.10	17.25	-4.0
Ge-2	1.1×10^{17}	0.241	3.90	17.3	-9.0
Si-1	2.5×10^{16}	0.22	7.7	10.20	+5.0
Si-2	7.5×10^{16}	0.23	7.7	9.23	+5.0

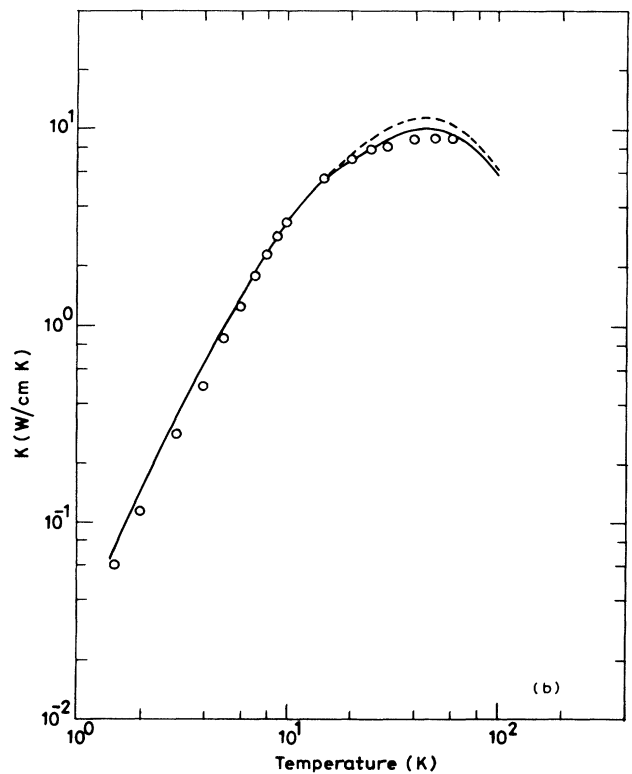
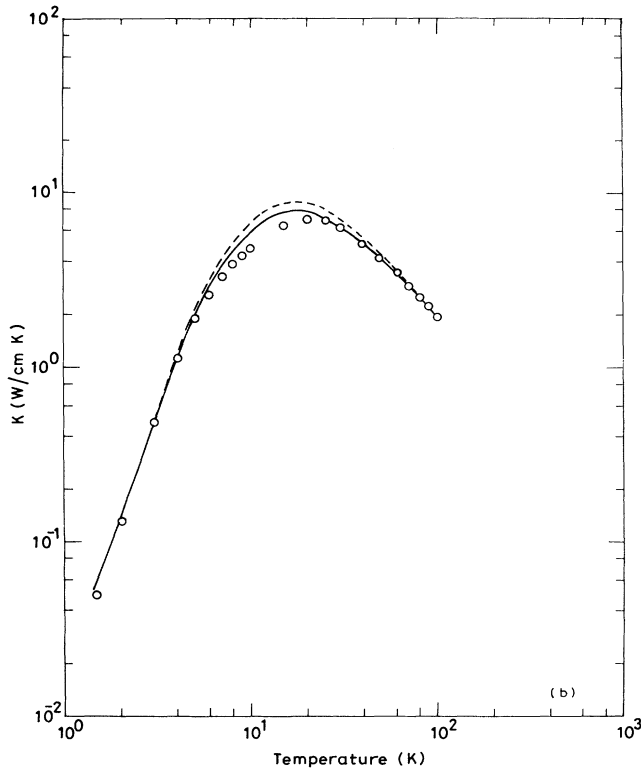
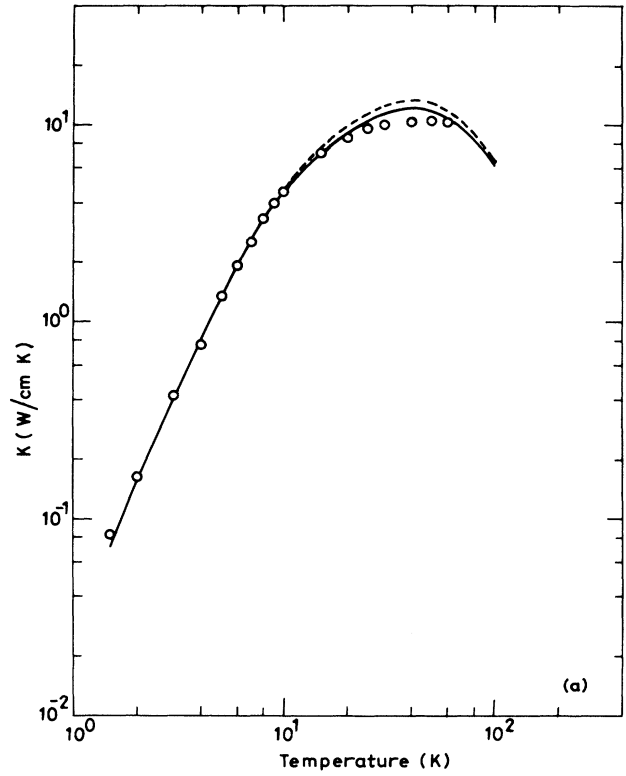
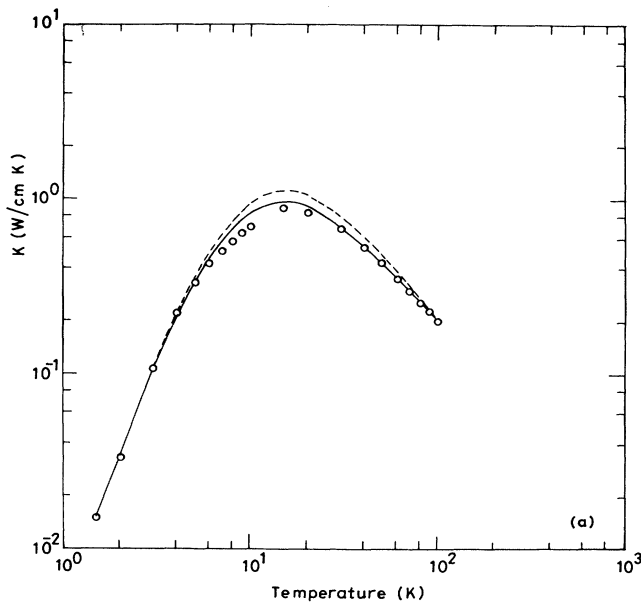


FIG. 1. Phonon conductivity obtained by the present calculations, the Suzuki and Mikoshiba (SM) (Ref. 7) theory and the experiment for As-doped Ge (a) Ge-1, (b) Ge-2. The solid line shows the present calculation; the dashed line is for the SM theory with $E_u = 15.13$ and 14.70 eV for samples Ge-1 and Ge-2, respectively, with $a^* = 36.69$ Å.

FIG. 2. Phonon conductivity obtained by the present calculations, the Fortier and Suzuki (FS) (Ref. 11) theory, and the experiment for Li-O-doped Si (a) Si-1, (b) Si-2. The solid line shows the present calculation; the dashed line is for the FS theory with $E_u = 10.36$ and 9.47 eV for samples Si-1 and Si-2, respectively, with $a^* = 17.16$ Å.

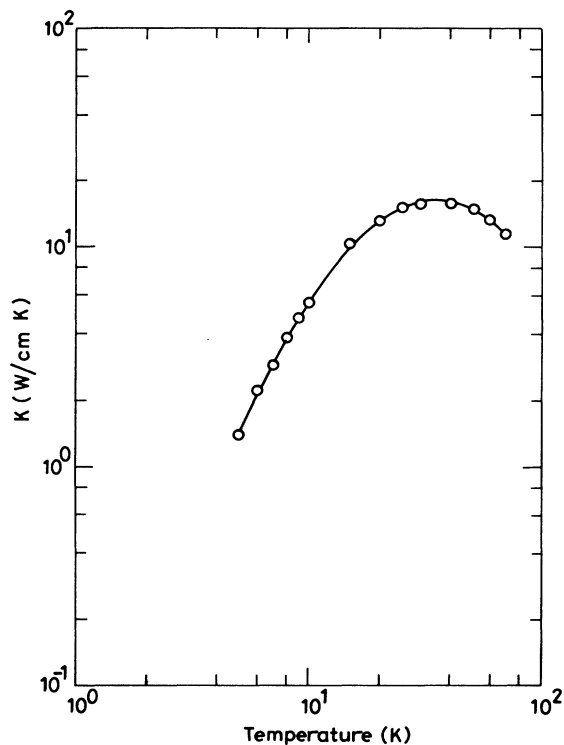


FIG. 3. Phonon-conductivity fitting obtained using the Holland model (Ref. 10) with the experimental value for Si containing oxygen $\approx 5 \times 10^{17} \text{ cm}^{-3}$.

phonon conductivity data caused a considerable amount of variation in its value. Therefore, considering the possible errors involved in the experimental data of the phonon conductivity and donor concentration, we can say that (Fig. 1) the present theory works remarkably well in case of As-doped Ge, particularly in between temperature limits 30–100 K and 2–5 K.

Experimental data for phonon conductivity of Li-O donors in Si has been provided by Fortier *et al.*¹² This case is much more complicated than As-doped Ge because oxygen centers having concentration $\approx 5 \times 10^{17} \text{ cm}^{-3}$ act as point defects to introduce extra phonon scattering. According to our estimate, the phonon-point defect parameter, by fitting the phonon conductivity data of the sample Si-I (Fig. 3) which contains oxygen but no Li, is found to be $= 8.0 \times 10^{-45} \text{ sec}^3$. Using this parameter, the phonon conductivity of samples doped with Li-O was adjusted. Figure 2 shows that the best fits are obtained for $E_d = +5 \text{ eV}$, while most of the works^{13,16} report its value to be $\approx -5 \text{ eV}$. It is interesting that in their theory, Cheung and Barrie⁵ also had to take its value $+11 \text{ eV}$ in an attempt to explain the shift in the donor energy levels with temperature. The exact choice of the parameters E_d and E_u in this case cannot be taken too seriously as phonon scattering by boundary is also very effective up to $T \approx 10 \text{ K}$. In fact, Figs. 4 and 5 show that τ_{e-ph}^{-1} and τ_{pt}^{-1} become effective only after $\omega \approx 10^{12} \text{ Hz}$. Consequently, a little variation in τ_B^{-1} or an introduction of any other scattering process, effective for phonons with frequency

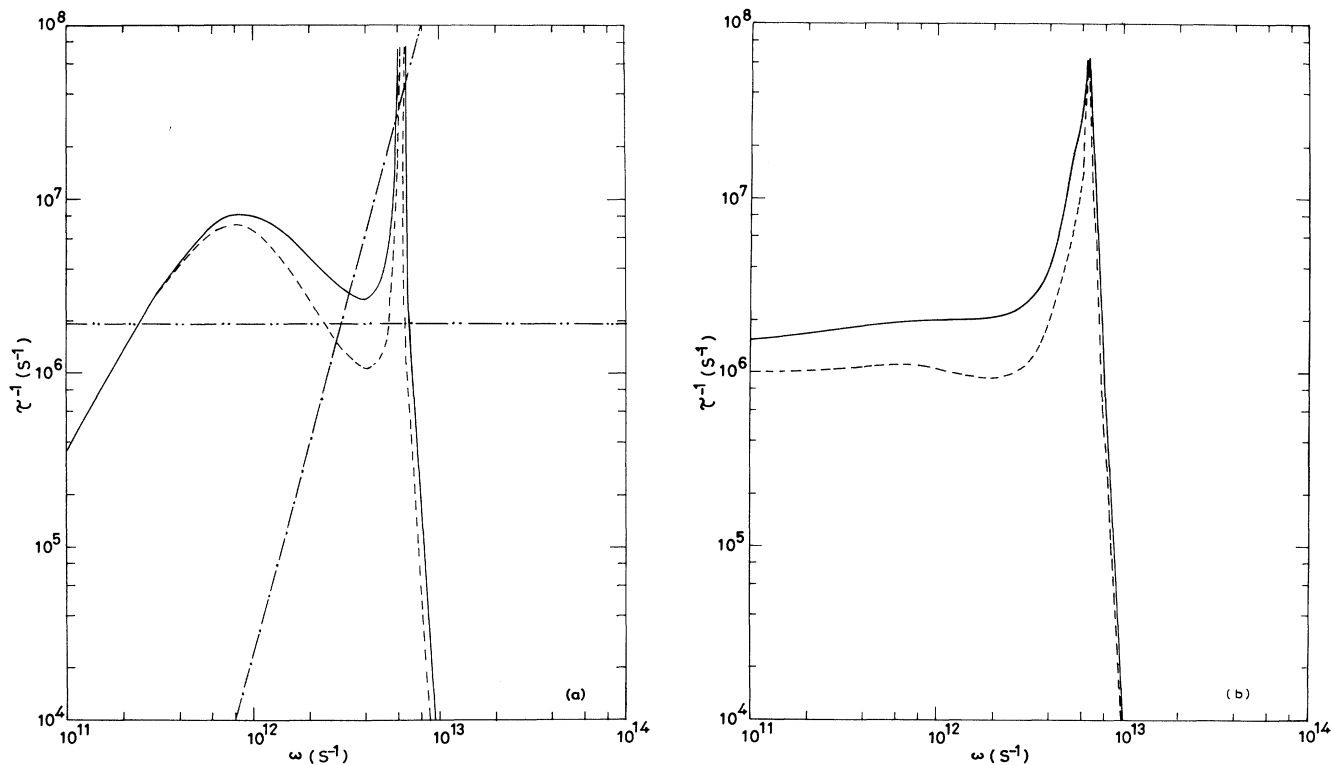


FIG. 4. Relaxation rates of the incoming longitudinal phonon as a function of angular frequency ω in Ge-1 at $T=20 \text{ K}$ with $E_u = 17.7 \text{ eV}$. (a) The solid line is for $E_d = -5 \text{ eV}$ and the dashed line is for $E_d = -8 \text{ eV}$. For elastic process; — · — is for boundary scattering; — · — is for the point defect scattering, (b) absorption process.

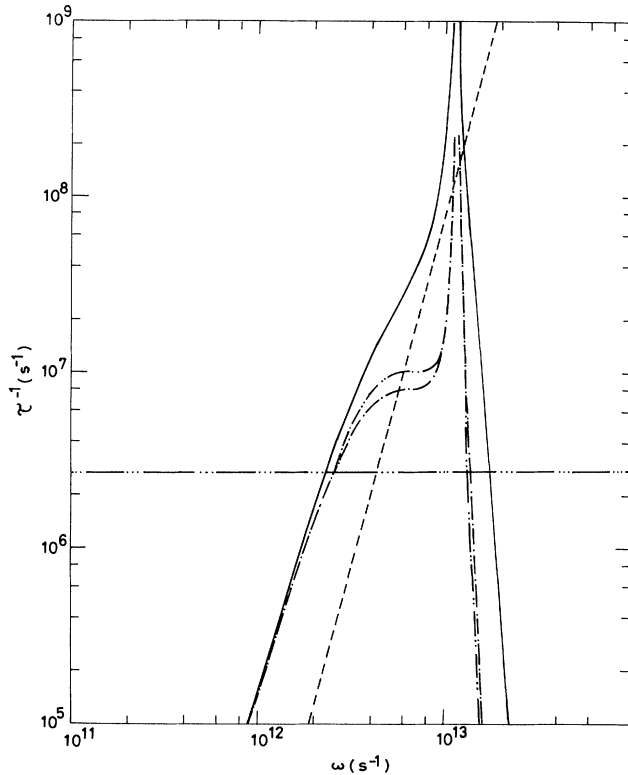


FIG. 5. Relaxation rates of the incoming longitudinal phonon as a function of angular frequency ω in Si-1 at $T=15$ K. — and — — represent $\tau^{-1}(el)$ from the present calculations with $E_d=5$ and -6 eV, respectively, and $E_u=11$ eV. — · — is from the SM theory $\tau^{-1}(el)$ with $E_u=11$ eV. — — — is for point defect, — · · — is for the boundary scattering.

$\leq 10^{12}$ Hz (e.g., phonon scattering due to the hopping process¹⁷), will immediately affect the parameters. The positive value of E_d would, however, still be required for the final adjustment.

It is to be noted from Figs. 1 and 2 that the anisotropy of the form factor allows a larger thermal resistance at higher temperatures not only via an increase in the cutoff

frequency, but also through the effect of the dilatation deformation potential on the phonon-electron interaction. Figures 4 and 5 make it clear that the dilatational part of the deformation potential, which can scatter longitudinal phonons only, plays a role which is much more important than anticipated by earlier works^{7,8,9,15} as well as in our previous paper.¹

Figures 1 and 2 reveal that the discrepancy between theory and experiment still exists around the phonon conductivity maxima in both Ge and Si samples. A possible explanation through the added phonon point defect scattering due to doping or the frequency-dependent deformation potentials, as suggested in our previous paper,¹ is now discluded as it would largely disturb the fitting at higher temperatures. The variation of 4Δ with N_{ex} (see Table II) as observed through Raman scattering¹⁸ in As-doped Ge also could not improve the theoretical results much. Similarly, an assumed splitting of even ± 0.3 meV of the triplet due to internal stress in As-doped Ge did not work. A larger splitting, in the presence of internal stress, seems to be improbable. Moreover, this conjecture^{19,20} is neither in line with the experimental studies of impurity states in unstressed As-doped Ge (Ref. 21) or Li-O-doped Si (Ref. 3) nor does it get support from the observations of phonon conductivity vs stress data.²² Further, the phonon resonances^{23,24} by localized impurity states usually occur at higher frequencies. The answer to this discrepancy may probably come from any of the following possibilities.

(i) The larger anisotropy of the donor wave function due to the strain field caused by the mismatch of impurity.

(ii) The interference effect between two types of phonon scatterings, e.g., the mass defect and electron phonon in this case, also needs careful investigation. Kumar and Ansari²⁵ have shown considerable effects of interference in between phonon scattering by dislocations and mass defect in plastically deformed LiF.

(iii) The existence of donor pairs,²⁶ due to some unintentional compensation, may give a weak but extra peak in τ_{e-ph}^{-1} vs ω at a somewhat lower frequency in Figs. 4 and 5. This may also very well account for the above-mentioned discrepancy in the present work.

*Permanent address: Department of Physics, University of Chittagong, Bangladesh.

¹M. K. Roy and K. C. Sood, Phys. Rev. B **44**, 11 085 (1991).

²J. F. Goff and N. Pearlman, Phys. Rev. **140**, A2151 (1965).

³R. L. Aggrawal, P. Fisher, V. Mourzine, and A. K. Ramdas, Phys. Rev. **138**, A882 (1965).

⁴W. Kohn, in *Solid State Physics*, edited by F. Seitz and D. Turnbull (Academic, New York, 1957), Vol. 5, p. 257.

⁵C. Y. Cheung and R. Barrie, Can. J. Phys. **45**, 1421 (1967).

⁶N. F. Miller and E. Abrahams, Phys. Rev. **120**, 745 (1960).

⁷K. Suzuki and N. Mikoshiba, J. Phys. Soc. Jpn. **31**, 186 (1971).

⁸P. C. Kowk, Phys. Rev. **149**, 666 (1966).

⁹A. Griffin and P. Carruthers, Phys. Rev. **131**, 1976 (1963).

¹⁰M. G. Holland, Phys. Rev. **132**, 2461 (1963).

¹¹D. Fortier and K. Suzuki, Phys. Rev. B **9**, 2530 (1974).

¹²D. Fortier, H. Djerassi, K. Suzuki, and H. J. Albany, Phys. Rev. B **9**, 4340 (1974).

¹³R. Ito, H. Kawamura, and M. Fukai, Phys. Lett. **13**, 26 (1964).

¹⁴K. Murase, K. Enjouji, and E. Otsuka, J. Phys. Soc. Jpn. **29**, 1248 (1970).

¹⁵A. Kumar, A. K. Srivastava, and G. S. Verma, Phys. Rev. B **2**, 4903 (1970).

¹⁶R. A. Stradling and V. V. Zhukov, Proc. Phys. Soc. **87**, 263 (1966).

¹⁷Z. W. Gortel, J. Phys. C **9**, 693 (1976); **9**, 707 (1976).

¹⁸J. Doehler, Phys. Rev. B **12**, 2917 (1975).

¹⁹K. Suzuki, Phys. Rev. B **11**, 3804 (1975).

²⁰M. Singh and G. S. Verma, Phys. Rev. B **118**, 5625 (1978).

²¹J. H. Reuszer and P. Fisher, Phys. Rev. **135**, A1125 (1964).

²²R. W. Keys and R. J. Sladek, Phys. Rev. **125**, 478 (1962).

²³David K. Brice, Phys. Rev. **110**, A1211 (1965).

²⁴F. L. Vook, Phys. Rev. **140**, A2014 (1965).

²⁵A. Kumar and M. A. Ansari, Physica B **147**, 267 (1987).

²⁶B. L. Bird and N. Pearlman, Phys. Rev. B **4**, 4406 (1971).